POTENTIAL ASSESSMENT AND INITIAL DESIGN FOR A FUEL AND NOISE REDUCING TRAJECTORY OPTIMISATION SYSTEM FOR TURBOPROP AIRCRAFT BASED ON ADS-B DATA

Joscha Kurz*, Christoph Deiler*
* German Aerospace Center (DLR), Institute of Flight Systems, Lilienthalplatz 7, 38108 Braunschweig, Germany

Abstract

The German Aerospace Center (DLR) has developed and successfully proved the Low Noise Augmentation System (LNAS) for turbofan aircraft. LNAS assists pilots with their speed and aircraft configuration management during approach in order to increase fuel efficiency, decrease noise exposure on ground, and being stabilised at 1000 ft above threshold elevation. The operation of turboprop aircraft differs from turbofan aircraft in the mission profile and the operating procedures. The flight performance is characterised by significantly lower cruise speeds and altitudes compared to turbofan aircraft. However, they are more fuel efficient and less maintenance demanding. These advantages result in lower operational costs and less CO_2 emissions that underline the relevance of turboprop aircraft more for the future. This paper describes the assessment of a potential benefit and the initial design of a similar trajectory optimisation system for turboprop aircraft. It further provides some basics about turboprop aircraft, the description of the recording and processing of broadcasted ADS-B data performed to gather simple flight data of approaching turboprop aircraft (Dornier 328-100). Afterwards, it describes the estimation of relevant flight parameters from processed data and the analysis regarding a potential to improve fuel efficiency and reduce noise. The recorded ADS-B data show a strong variation in altitude and speed profiles with track distance. Furthermore, the calculated derivations of the aircraft's total energy indicate an energy supply which is likely caused by the engine power lever. These findings in ADS-B data suggest the presence of an optimisation potential to improve the energy management of turboprop aircraft during approach. In addition, the findings are supported by the availability of a small number of high-quality flight test data from DLR's UpLift Dornier 328-100 research aircraft (D-CUPL). Lastly, this paper describes and discusses the initial concept of an appropriate optimisation system, including the design of corresponding cockpit display indications that are needed to assist the cockpit crew during approach. Research on the described concept of trajectory optimisation and its realisation is being continued at DLR in order to contribute to sustainable aviation in the future.

Keywords

turboprop aircraft, trajectory optimisation, aircraft noise, fuel efficiency

NOMENCLATURE

Symbols

α	angle of attack	deg
α_w	wind angle of attack	deg
C_D	drag coefficient	-
C_L	lift coefficient	-
E	energy	J
e	specific energy	J/kg
F	force	N
γ	flight path angle	deg
g	gravity	m/s^2
H	height	m
m	mass	kg
ϕ	roll angle	deg
q	dynamic pressure	Pa
S	wing area	m^2
θ	pitch angle	deg
t	time	s
TQ	engine torque	%
V	velocity	m/s
V_{FE}	maximum flap extended speed	kt
V_{LE}	maximum landing gear extended speed	kt
V_{LO}	maximum landing gear operating speed	kt
V_{REF}	reference speed	kt

Indices

0	initial state
12	flaps 12°
20	flaps 20°
32	flaps 32°
a	aerodynamic
D	drag
in	in
L/G	landing gear
Ldg	landing

CC BY-NC-ND 4.0

doi: 10.25967/650036

out	out
T	thrust
TQ	torque

Abbreviations

AAL	Above Aerodrome Level
ADS-B	Automatic Dependent Surveillance Broadcast
ATC	Air Traffic Control
CAS	Calibrated Air Speed
DLR	German Aerospace Center
EFB	Electronic Flight Bag
EICAS	Electronic Indicating, Caution, and Advisory System
FAF	Final Approach Fix
FL	Flight Level
IAF	Initial Approach Fix
ICAO	International Civil Aviation Organization
ILS	Instrument Landing System
LNAS	Low Noise Augmentation System
MFD	Multifunction Display
MSL	Mean Sea Level
PFD	Primary Flight Display
RNP	Required Navigation Performance
STAR	Standard Terminal Arrival Routes
TQ	Torque
VAPP	Final Approach Speed
V/S	Vertical Speed

1. INTRODUCTION

The European Aviation Environmental Report 2025 expects that the total number of arriving and departing flights is going to grow to 9.9 million flights in 2030 and 11.8 million in 2050 for the most-likely base scenario by using airports of the 27 member states of the European Union and the European Free Trade Association, compared to the level of 9.2 million in 2019 [1]. Increasing public awareness of global climate change and the health effects of noise indicate that ecological aspects and aircraft noise become more meaningful besides economic efficiency. Aircraft noise exposure affects the health and wellbeing as for example in the form of stress caused by the annoyance, sleep disturbance, heart disease, premature mortality due to ischaemic heart disease, and learning impairment to children [2]. Furthermore, it has been shown that residents feel more annoyed by aircraft noise than that caused by other transport sources [3]. The World Health Organization (WHO) recommended in 2018 to implement measures to reduce the day-evening-night noise level below 45 dB, as higher levels are associated with adverse health effects. During night time the WHO recommended to reduce noise exposure below 40 dB, as higher levels are associated with adverse effects on sleep. [4] The objectives of the European Commission's *Flightpath 2050* agreement are to reduce CO_2 emissions per passenger kilometre by 75%, NOx emissions by 90%, and perceived noise by 65% by 2050 compared to the capabilities of a typical new aircraft in 2000 [5]. The Balanced Approach of the International Civil Aviation Organization (ICAO) encompasses four principle elements to address aircraft noise problems where they occur, for an individual airport-by-airport approach: reduction of noise at source, land-use planning and management, noise abatement operational procedures, and operating restrictions on aircraft [6]. The development and implementation of new aircraft or low-noise technology modifications (e.g., fairings, acoustic liners, low-noise fan, chevron nozzle) – to reduce noise usually at the source – generally takes time. Noise abatement operational procedures, such as noise preferential routes, standard instrument departures, standard terminal arrival routes (STAR), dispersed flight tracks, automated procedures, noise preferential runways, displaced thresholds, or noise abatement departure and approach procedures [6], have the benefit that they can provide short- to mid-term solutions for reducing the noise exposure at certain locations. These noise abatement operational procedures mentioned as examples are already implemented and in service but are also continuously observed and adjusted, e.g., to new research results or individual local needs and constraints around an airport. Furthermore, such operational measures have the notable advantage that aircraft with an aged technical level are also able to apply those measures. This is beneficial, because those aircraft are still in service and usually emit more noise at the source compared to new aircraft. Further noise reduction and fuel efficiency may be achieved by the optimisation of aircraft's energy management and providing corresponding systems. This paper focusses on the optimisation of the vertical flight trajectory of an aircraft by an assistance system that optimises the aircraft's energy management and assists the cockpit crew during descent and approach. This helps to fly the optimised approach procedure precisely, which can result in an increased flight height above the ground, reduced aerodynamic drag, and/or less engine power. Furthermore, the optimisation can continuously adjust the aircraft's energy management to changing conditions (e.g., new air traffic control (ATC) instructions, wind speed and direction). Consequently, fuel consumption and noise levels on ground can be reduced, and the system an also help to minimise the risk of an unstable approach.

2. AIRCRAFT TRAJECTORY OPTIMISATION

2.1. DLR's Low Noise Augmentation System

During the last decade, the German Aerospace Center (DLR) developed, tested and matured the Low Noise Augmentation System (LNAS) for the Airbus A320 family, which optimises the vertical flight trajectory of turbofan aircraft [7–9]. The system continuously optimises the vertical flight trajectory between the top of descent and the stabilisation height shortly before landing. In the case of events that cause the aircraft to deviate from the previously optimised trajectory (e.g., pilot inputs deviating from the previous optimisation, new ATC instructions, changed wind conditions), the LNAS optimisation algorithm takes the deviation and the new boundary condition into account

CC BY-NC-ND 4.0



FIG 1. LNAS running on the electronic flight bag of an Airbus A320 showing the vertical situation display and the status bar on top; credit: DLR (all rights reserved).



FIG 2. DLR's UpLift Dornier 328-100 research turboprop aircraft; credit: DLR (CC BY-NC-ND 3.0)

accordingly and updates the trajectory. Designed as an external advisory system, LNAS provides recommendations for pilot actions for airspeed settings, vertical flight modes, and aircraft configuration management by appropriate cues on a display for a specific approach procedure. These cues are currently displayed on the Electronic Flight Bags (EFB) using a bar display containing all required pilot actions and an additional vertical situation display just to provide more information to the cockpit crew (Fig. 1). In future, it is planned to integrate the LNAS core in the primary aircraft avionics and display the pilot action cues directly in today's cockpit displays (i.e., primary flight display (PFD), navigation display (ND)). LNAS has successfully proven by several research test campaigns using the flight simulator and research aircraft, and during extensive flight trials during daily airline operations. The results show that LNAS significantly increases fuel efficiency, decrease noise exposure on ground, and ensures being stabilised at 1000 ft AAL (Above Aerodrome Level) [10–14].

2.2. Problem definition

Turboprop aircraft are propeller driven aircraft powered by a turbo-engine. The turbo-engine is generally assembled by a high-pressure-compressor, a combustion chamber, and a high-pressure-turbine that provides mainly rotational power to the propeller via a shaft and a gearbox [15]. The turbo-engine produces only a small amount of thrust by the exhaust gases of the turbo-engine compared to a turbofan aircraft [15]. Taking into account this difference, the turbo-engine works basically the same way as the core engine of a turbofan aircraft. The main thrust, however, is produced by the propeller, which converts the rotational power from the turbo-engine into propulsion power. The propeller is open and without a coating which is typically used for the fan of turbofan-engine. As the propeller efficiency decreases significantly with increasing airspeed, turboprop powered aircraft are normally operated at speeds up to Mach 0.7 [15]. The specific fuel consumption of turboprop-engines is comparatively lower than for turbofan-engines [15]. The differences in the propulsion directly affect flight performance and the mission profile of turboprop aircraft. For short range flights, the operating costs of turboprop aircraft are less than for turbofan aircraft. Furthermore, due to the high propulsive efficiency at low airspeeds, smaller turboprop aircraft usually require a shorter runway field length for take-off than turbofan aircraft. At the same time, the ground effect during landing is lower and the flare distance shorter for high-wing aircraft, which is a quiet common design for large turboprop aircraft. These effects on the take-off and landing distances also allow to operate the aircraft at more (regional) airfields. The environmental aspects in terms of burnt fuel and CO_2 emitted are also of interest for future aviation.

However, today the automation level and accordingly the cockpit procedures of old regional turboprop aircraft differ from (mostly further developed) turbofan aircraft: the availability of autopilot and auto-throttle functions is limited. For example, the Dornier 328-100 (Fig. 2) is not equipped with an auto-throttle system for which reason airspeed needs to be controlled manually by the cockpit crew. The engines are controlled by a power lever to control engine torque and a condition lever to control propeller speed [16]. Additionally, the aircraft is not equipped with speed brakes that could be used to decelerate quickly [16]. With increasing popularity of turboprop aircraft, differences in the automation level and also energy-efficient systems between turboprop and turbofan aircraft might become smaller.

As turbofan aircraft constitute the majority of operating turbofan and turboprop aircraft [1], also research seems to has focussed largely on this type of aircraft. The availability of research on turboprop aircraft is less and literature, useful information, and aircraft-specific data are very limited. Due to the importance of turbofan aircraft to date, DLR also intends to place a stronger focus on turboprop aircraft in the future and gain more experience with their operation and the associated research topics. Since the effects of aircraft noise and its assessment are always an important element in research on approach and departure procedures, the calculation of noise impact and the noise reduction potential is a highly relevant topic that require more dedicated research and developments. DLR has now started researching on a trajectory optimisation system that targets on an energy-efficient descent and approach of turboprop aircraft. At the same time, it is anticipated that this energy-efficient approach will also reduce aircraft noise during this phase of flight. The proposed trajectory optimisation system could be integrated as a software solution in both, new and old turboprop aircraft, to increase efficiency and reduce aircraft noise.

[1] Flightradar24 Live Air Traffic. URL: https://www.flightradar24.com

CC BY-NC-ND 4.0

3. FLIGHT DATA ANALYSIS

3.1. Method

For the analysis of the approach optimisation potential of turboprop aircraft, ADS-B data of approaches at Braunschweig-Wolfsburg Airport (EDVE) were used. These were mainly tracked by six Air!Squitter receivers around the airfield. The Jetvision Air!Squitter [2] receiver allows live flight tracking of ADS-B (Automatic Dependent Surveillance-Broadcast), MLAT (Multilateration), and FLARM (Portable Collision Avoidance System) signals. The received ADS-B signals of approaching Dornier 328-100 aircraft were recorded between June and September 2024 and the data from a total of 101 flights were processed and analysed. These ADS-B data contain a limited number of parameters, whereby the relevant parameters – in addition to aircraft type and registration – are

- time,
- barometric altitude,
- longitude and latitude,
- true track angle,
- speed over ground, and
- vertical speed [3].

The ADS-B data were processed and other important operational parameters (e.g., indicated airspeed, altitude) were estimated and calculated. The atmospheric conditions were estimated using the Copernicus Climate Data Store ERA5 weather model [17], which provides, among many other parameters, the geopotential height, wind speed components, and temperature for a specific location and at different pressure altitudes in the past. The historically modelled weather data appear to be sufficiently accurate, as the parameters calculated from them fulfil typical values for certain flight phases (e.g., calibrated airspeed of 250 kt below FL100).
Feedback from discussions with turboprop pilots was taken into account when exploring the optimisation potential and defining the subsequent flight path optimisation concept in Chapter 4.
Furthermore, the concept definition utilised aircraft manuals available to DLR (Airplane Flight Manual [18], Airplane Operating Manuals [16, 19], Quick Reference Handbook [20]). The Airplane Flight Manual provides – among other contents – information about the aircraft in general, the operational limitations, the flight procedures, and the flight performance during individual flight phases. The Airplane Operating Manuals describe the operation of the aircraft and its systems, and provide performance data for flight planning purposes. The Quick Reference Handbook provides checklists for normal procedures as well as procedures for abnormal situations.
Noise measurement data were not available for a noise assessment. Furthermore, the available ADS-B data did not include any information about engine performance or aircraft configuration. Both have a significant influence on noise emissions at the aircraft and thus also on noise impact on ground. Other more detailed operational flight data including pilot inputs were also not available. A rudimentary quantitative noise assessment was therefore not considered useful and was not pursued further. The qualitative discussion of the flight performance observation in ADS-B data had to be sufficient.

[2] Günter Köllner Embedded Development GmbH. Air!Squitter. URL: https://airsquitter.com/ (Accessed: 06.05.2025)
[3] Jetvision Support Wiki. URL: https://wiki.jetvision.de/wiki/Radarcape:Software_Features Accessed: 08.09.2025)

3.2. Results

Figures 3 to 6 show the results of the ADS-B data analysis for a total of 101 approaches to Braunschweig-Wolfsburg Airport (EDVE). The parameters altitude, calibrated airspeed, vertical speed, and change in specific energy are plotted over the track distance to threshold. The runway threshold is at 0 NM. The approaches from the west on runway 08 using an RNP approach (Required Navigation Performance) are shown in cyan, while the approaches from the east on runway 26 performing an ILS approach (Instrument Landing System) are shown in black.
In Figure 3, the RNP approaches indicate a significantly lower dispersion in altitude compared to ILS approaches. The RNP approaches show continuous descending flights, whereby the flight altitude is higher on average. Horizontal flight segments can only be recognised for the instrument approaches. The continuous descent during RNP approaches is presumably due to the flight guidance mode, in which the autopilot guides the aircraft along space vectors between the route waypoints of the instrument approach.

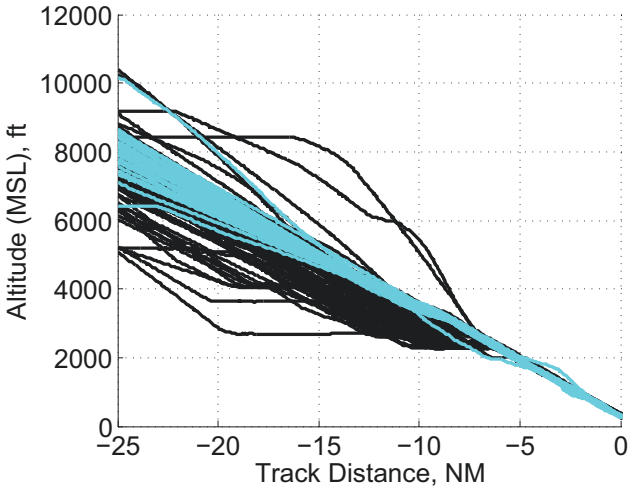


FIG 3. Altitude profiles for runway 08/26 (cyan/black) at Braunschweig-Wolfsburg Airport (EDVE)

Figure 4 shows a clear dispersion in the calibrated airspeeds for both approach directions. Up to a distance of about 7 NM to the runway threshold, the airspeeds scatter by almost 100 kt. Starting at a distance of about 5 NM to the runway threshold, the airspeeds and their dispersion decrease significantly and remain almost constant. This is just before the range below an altitude of 1000 ft AAL at around 3 NM, from which the aircraft is probably configured for landing, the final approach speed is reached, and the approach should therefore be stabilised. It can also be seen that the airspeed curves of the individual approaches are not decreasing monotonously, rather noticeable increases can be observed during the descent.
The vertical speed in Figure 5 does also contain a significantly lower variation for the RNP approaches compared to the ILS approaches. In addition, the figure visualises the missing of horizontal flight segments in the RNP approaches from a distance of around 22 NM to the runway threshold.
Figure 6 shows the change in the specific total energy $\dot{e}_a$, consisting of specific potential and kinetic energy (Eq. 1). If the change in the total energy takes on positive values, an

CC BY-NC-ND 4.0

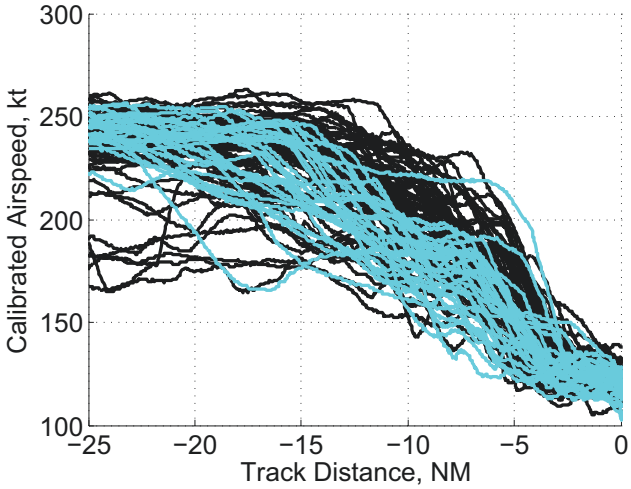


FIG 4. Airspeed profiles for runway 08/26 (cyan/black) at Braunschweig-Wolfsburg Airport (EDVE)

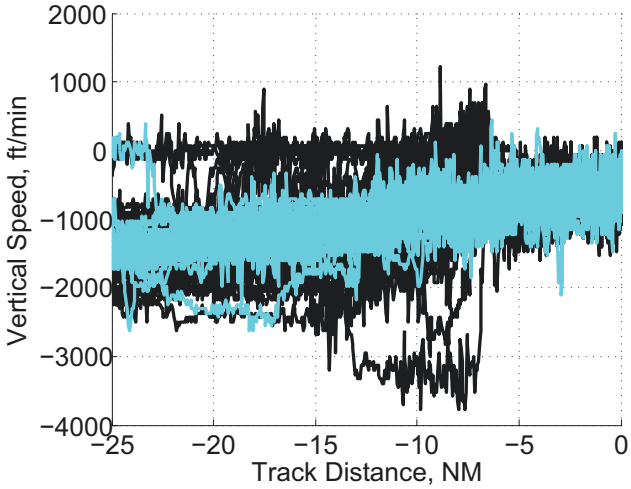


FIG 5. Vertical speed profiles for runway 08/26 (cyan/black) at Braunschweig-Wolfsburg Airport (EDVE)

energy supply must take place.

$$e_a = \frac{E_a}{m} = g\,H + \frac{V_a^2}{2} \qquad (1)$$
$$\dot{e}_a = \frac{de_a}{dt} = g\,\dot{H} + V_a\,\dot{V}_a$$

As the calculation of the kinetic energy is based on the true airspeed, which already takes the mean wind into account, it is unlikely that the mean tailwind has an influence as an energy input. However, the wind data used does not contain information of local wind gusts, which is why these could still have an influence on the calculated true airspeed and kinetic energy. Since the airspeed fluctuations are rather slow, oscillate only slightly, and a general trend in airspeed is recognisable (see Fig. 4), it is nevertheless assumed that the aircraft was mainly supplied with energy by the movement of the power lever and thus by the engines.

This assumption is supported by a small number of engine torque signals from operational flight data of DLR's Dornier 328-100 (D-CUPL) shown in Figure 7. It must be noted that these data contain 11 arbitrary approaches which were recorded during flight test campaigns and not during commercial airline operation. Hence, these data are not evaluated in more detail in direct relation to the analysis presented, to not bias the results. Nevertheless, it is still

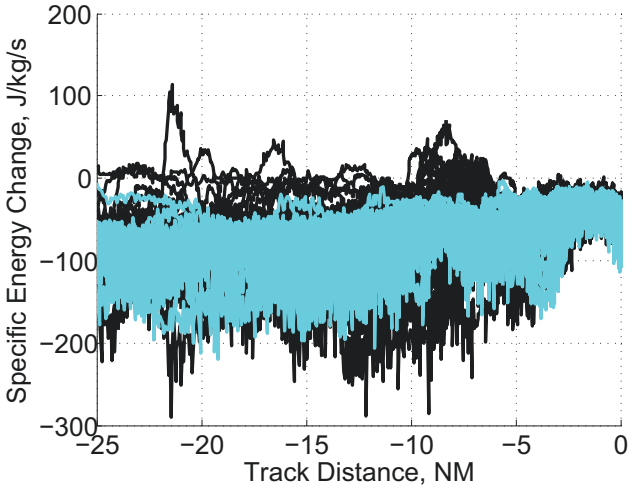


FIG 6. Total specific energy change profiles for runway 08/26 (cyan/black) at Braunschweig-Wolfsburg Airport (EDVE)

clearly recognisable that there are high gain inputs through the power lever to control the engines respectively propeller thrust to adjust the aircraft energy and airspeed. Of course, the power lever could also have been moved to compensate for wind gusts, which cannot be equalised manually as quickly as would be possible with an auto-throttle.

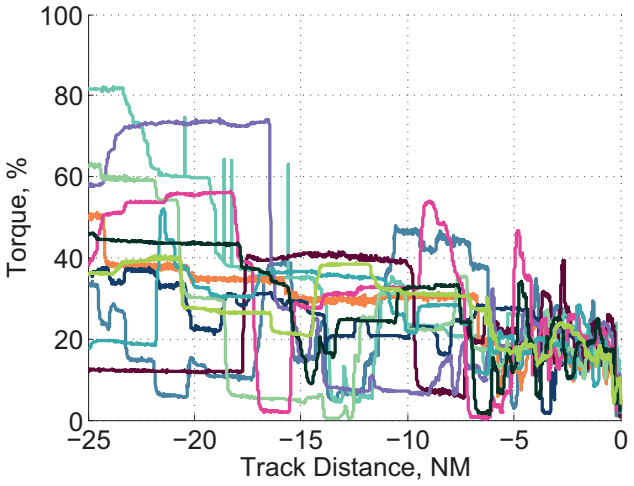


FIG 7. Engine torque signal of 11 approaches (Dornier 328-100)

The ADS-B data analysis shows that there are large variations between the flight trajectories, particularly in the airspeeds. The airspeed profiles show also clear fluctuations along the track distance. Therefore, potential for improved energy management seems to exist. Given the fact, that there is no auto-throttle or speed controller available for the Dornier 328-100 and airspeed is controlled manually by the cockpit crew, it can be assumed that potential for practical improvement in flight operations is limited. The data reveal that during some approaches too much energy was dissipated too early, which resulted in an additional need for energy at a later stage of the flight. At the same time, it can be seen that for a few approaches a significant amount of energy was dissipated very late.

For continuous deceleration and energy reduction, optimised speed and aircraft configuration management is required avoiding the need for thrust increase during the approach and hence power lever use. This further includes the adjustment of the top of descent (prior to the approach) and the deceleration point. The optimisation could relieve

CC BY-NC-ND 4.0

the cockpit crew during the approach and also reduce the risk of high energy and unstable approaches.
On average, the implementation of a corresponding system can be expected to improve energy management, reduce the variation in airspeed, and thus reduce fuel consumption. This suggests that high-energy approaches can be avoided, especially on the final approach, which tend to be particularly noisy, as aircraft are at low altitudes and the excess energy has to be corrected by setting the flaps and extending the landing gear early. These expectations have already been confirmed during the testing of a comparable pilot assistance system for turbofan aircraft [9, 10].
In addition, the implementation of an auto-throttle could help to improve stability in airspeed, avoid overcompensations, and provide a further potential to reduce fuel consumption and engine noise.
It must be stated, that ATC requirements could not be considered for this evaluation but have a major influence on flying an energy-optimised approach. Nevertheless, the anomalies that indicate potential for improvement in energy management are generally assessed as existing, e.g., even without ATC specifications. The energy optimisation algorithm of the proposed system needs to be capable to adjust the vertical trajectory, and the speed and configuration management to new specifications or situations (e.g., current airspeed and altitude, pilot inputs deviating from the previous optimisation, new ATC instructions, changed wind conditions).

4. TRAJECTORY OPTIMISATION

The trajectory optimisation consists of a vertical trajectory algorithm and an energy management algorithm.
The vertical trajectory algorithm calculates the vertical flight profile based on a sequence of waypoints and altitude constraints for a selected approach procedure (RNP). The algorithm provides the geometric flight path angle which is needed as an input for the energy management algorithm. The vertical trajectory is continuously updated accordingly to the actual aircraft position. It is geometrically adapted to the waypoints and altitude restrictions ahead, but there is no optimisation of the vertical trajectory in terms of considering the flight performance of the aircraft. The energy management algorithm consists of a reverse flight simulation to calculate and optimise the airspeed profile for approaching with minimum engine power along the given vertical trajectory and being stabilised at the stabilisation height (commonly 1000 ft AAL). This includes the calculation and re-optimisation of the aircraft configuration points (i.e., flaps and landing gear) and their adjustment due to deviations during approach. Additionally, the algorithm provides the outputs (i.e., pitch angle and engine torque) required to fly the optimised trajectory manually without an autopilot. Both algorithms are described in more detail in Section 4.1 and 4.2.
The principle of the optimised vertical trajectory is visualised in Figure 8, including the airspeed profile (during descent and approach) for continuous deceleration between top of descent and runway threshold, as well as the specific waypoints for deceleration and aircraft configuration. The configuration points are continuously adjusted, in direction of flight if the total energy is too low and in the opposite direction of flight if the total energy is too high, taking into account the operational airspeed limits for each aircraft configuration (i.e., flaps, landing gear), as sketched in the figure.
Figure 9 describes the sequence of the reverse simulation and how it is connected to the vertical trajectory algorithm. The reverse calculation starts with the latest vertical trajectory and environmental conditions (i.e., wind speed and direction, air temperature, air pressure) given, from which the geometric target path angle can be taken for each point along the flight path. Using flight mechanics equations approximating the aircraft motion, the flight conditions, and flight performance data, the aircraft motion can be calculated (or integrated) backwards: in the backwards calculation from touchdown to the current aircraft state (altitude and speed) the aircraft motion is reversed in the way, that a deceleration in positive time will be an acceleration in the backwards calculation. Or to put in other words, the time direction is changed, which means the time direction in the reverse simulation points in the opposite direction to the runway. Hence, in the backwards calculation altitude and speed are increased from touchdown to the current flight condition (ultimately top of descent). The pitch angle (θ) and engine torque (TQ) are an output of the reverse simulation and relevant parameters for the cockpit display indications, which help the cockpit crew to fly the optimised flight trajectory.

4.1. Vertical trajectory algorithm

The approach procedure is defined by a sequence of waypoints with associated altitude constraints, which are basically linearly connected. Figure 10 illustrates the approach trajectory computation process. First, altitude constraints along the calculated trajectory are considered. There are three types of altitude constraints. One type of constraints demands the aircraft passing a fix or a track to fix at a specified mandatory altitude ("at"). The other two types of constraints require the aircraft passing a fix or a track to fix at or above/below the specified altitude ("at or above","at or below"). The remaining distance to threshold is split into linear segments between the waypoints with mandatory altitude constraints ("at") for a fix or a track to fix. The 50 ft above threshold, the stabilisation height, and the final approach fix (FAF) are considered like mandatory altitude constraints. In Fig. 10, waypoints with mandatory altitude constraints are "IAF" ("@A5000"), "FAF" ("@A3000"), "1000 ft" ("@AAL1000"), and "THR" ("@AAL50"). Then, the algorithm checks all remaining altitude constraints. If they are not already fulfilled by the previously determined segments, the linear segments are adjusted accordingly at each waypoint to the minimum required altitude ("at or above") or the maximum allowed altitude ("at or below"). In Fig. 10, "at or above" altitude constraints (track to fix) are between "WP1" and "IAF" ("A5000+"), between "IAF" and "WP2" ("A4000+"), and between "WP2" and "FAF" ("A3000+"). After adjusting the trajectory to altitude constraints, the linear segment between top of descent and the first altitude constraint is left. This segment is initially considered as an extension of the subsequent segment. Next, the deceleration point is calculated by the energy management algorithm described in Section 4.2. The deceleration point can either be 1) between the previously determined segments (in Fig. 10, between "WP2" and "FAF" on the black trajectory) , 2) on the extended segment between the intersection point of the current aircraft altitude with the extended segment and the first altitude constraint (in Fig. 10, between top of descent and "FAF" on the yellow trajectory), or 3) before the intersection point with the extended segment at the current aircraft flight altitude. If the aircraft is at cruise altitude, the so called intersection point is equal to the top of descent. Finally, in the first two and also more common cases (used in Fig. 10), the intersection

CC BY-NC-ND 4.0

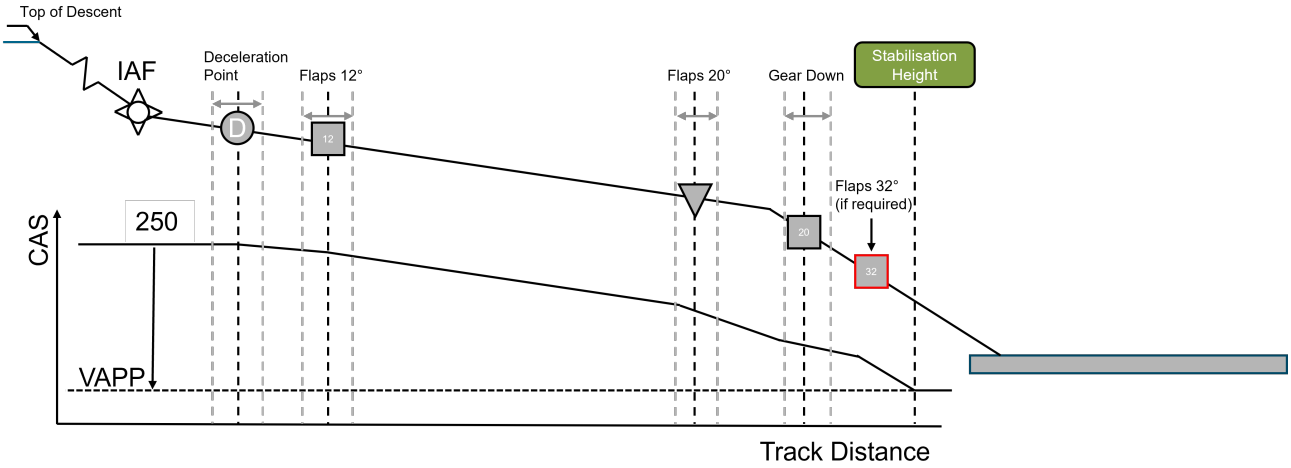


FIG 8. Schematic sequence of the system function between top of descent and runway threshold, including the vertical profile (top) and airspeed profile (bottom) (both not to scale)

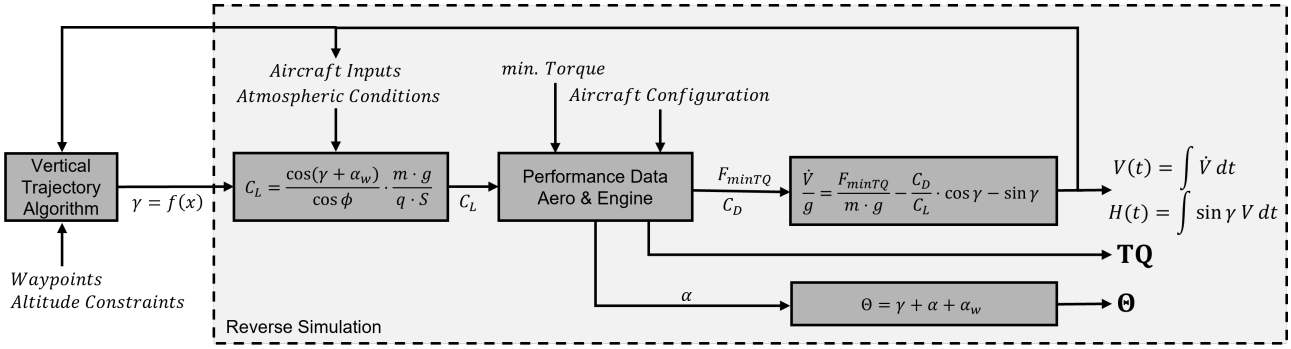


FIG 9. Schematic sequence of the backward calculation for a given vertical trajectory, including engine torque (TQ) and pitch angle (θ) for the cockpit displays

point (or top of descent) is determined by an averaged flight path angle for a descent with minimum engine power at constant airspeed to the first altitude constraint. Else, the deceleration point is before the intersection point (or top of descent), which connects the extended segment and the current aircraft altitude (not used in Fig. 10). The top of descent is considered as a waypoint with a mandatory altitude. In the end, all altitude constraints are met and the whole approach trajectory is described by waypoints and linear segments which are characterised by averaged flight path angles. In the case that there is no altitude constraint, the deceleration point is on the extended glideslope and is linearly connected with the top of descent by a segment for a flight path angle allowing a steady descent with minimum engine power (continuous descent operation).

4.2. Energy management algorithm

The tracking and management of the total energy during the approach allows to assess the energy state of the aircraft and – if necessary – to recommend actions to adjust the energy management and thus also to correct the total energy level. The total energy is the sum of potential energy and kinetic energy (Eq. 2).

$$E_a = m\,g\,H + \frac{1}{2}\,m\,V_a^2 \tag{2}$$

As airspeed and altitude are defined at fix waypoints (e.g., deceleration point, stabilisation height), the total energy management can be calculated and adjusted, using aerodynamic and engine data, to meet these values with as less engine power as possible. The difference in total energy between the stabilisation height ($E_{a,Ldg}$) and any initial waypoint along the flight trajectory ($E_{a,0}$), is equal to the sum of the energy added (E_{in}) and energy dissipated (E_{out}) in between (Eq. 3). These total energy changes correspond to the engine power applied (E_{in}) and the aerodynamic power loss (E_{out}) for a period of time. The engine power applied is integrated over the entire time between the initial waypoint and stabilisation height (Eq. 4). The aerodynamic power loss is the sum of the integrations of the aerodynamic power loss over time for all aircraft configurations, as the aerodynamic drag changes significantly for the same lift (Eq. 5):

- clean ($t_0 \rightarrow t_{12}$),
- flaps 12° ($t_{12} \rightarrow t_{L/G}$),
- flaps 12° & gear down ($t_{L/G} \rightarrow t_{20}$),
- flaps 20° & gear down ($t_{20} \rightarrow t_{32}$), and
- flaps 32° & gear down ($t_{32} \rightarrow t_{Ldg}$).

$$E_{a,Ldg} = E_{a,0} + E_{in} - E_{out} \tag{3}$$

$$E_{in} = \int_{t_0}^{t_{Ldg}} cos(\alpha)\, F_T\, V_a\, dt \tag{4}$$

CC BY-NC-ND 4.0

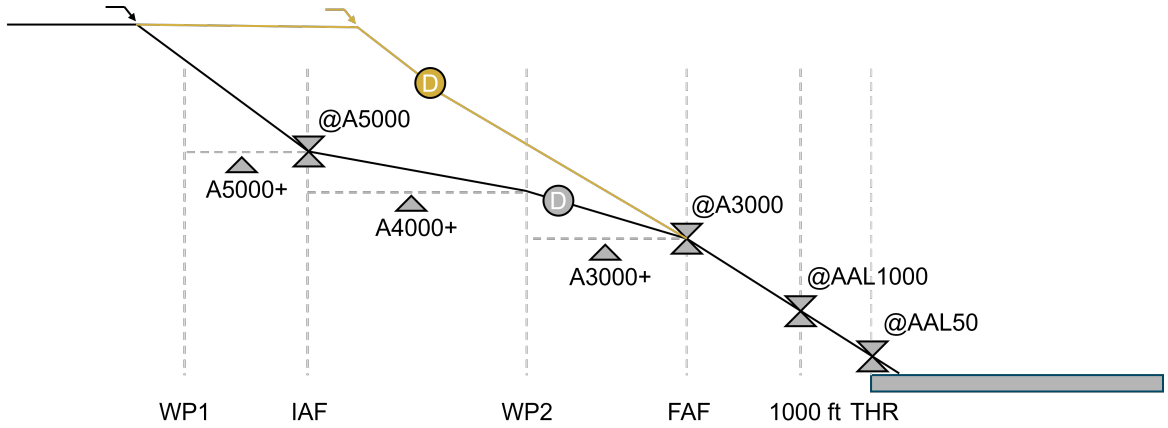


FIG 10. Exemplary approach trajectories considering altitude constraints (e.g., A4000+ "at or above") and mandatory altitude constraints (e.g., @A3000 "at"), deceleration point, and top of descent (not to scale)

$$
\begin{aligned}
E_{out} = & \int_{t_0}^{t_{12}} F_{D,0}\, V_a \, dt \\
& + \int_{t_{12}}^{t_{L/G}} F_{D,12}\, V_a \, dt \\
& + \int_{t_{L/G}}^{t_{20}} (F_{D,12} + \Delta F_{D,L/G})\, V_a \, dt \\
& + \int_{t_{20}}^{t_{32}} (F_{D,20} + \Delta F_{D,L/G})\, V_a \, dt \\
& + \int_{t_{32}}^{t_{Ldg}} (F_{D,32} + \Delta F_{D,L/G})\, V_a \, dt
\end{aligned}
\tag{5}
$$

The difference in total energy change, i.e., between the propulsive and the aerodynamic power, can be described in any reference systems [21], either using the true airspeed or the flight path velocity.

During real flight operations, the actual total energy of the aircraft along the flight path deviates from the initial calculation. At each position along the vertical flight trajectory the difference between the actual and the initially predicted aircraft energy level is known. This is caused by, e.g., differences in the predicted and actual wind speed and wind direction, new ATC instructions, or cumulated small model deviations. Within the energy management, the initial optimised approach trajectory and recommendations for pilot actions are re-optimised accordingly. The moments or positions for deploying flaps and landing gear, the deceleration point, and the top of descent are dynamically shifted forward and backward depending on the total energy loss rate required while applying as less engine power as possible. Within the permissible speed ranges, for example, the flaps and landing gear can be extended a little earlier if the total energy is too high or a little later if the total energy is too low, in order to successfully fly a stable approach with the lowest possible engine power. If the total energy gets too low, additional engine power may be required. The appropriate selection of the adjusted terms (Eq. 4-5) considers on various factors such as operational airspeed limitations, energy change potential of all segments for each aircraft configuration (i.e., flaps, landing gear), the resulting scope for further corrections, as well as the effect on fuel consumption and noise.

Figure 11 to Figure 13 visualise the principle of the adjustment of the configuration speeds for flaps and landing gear for the aircraft type Dornier 328-100. This example is based on a continuous descent starting at 10,000 ft at around 30 NM, with a flight path angle of -3°. As a reverse simulation is used, the configuration points for the landing gear and flaps 20° are adjusted first and for flaps 12° afterwards. The initial calculation (—) for the adjustment of the landing gear and flaps 20° starts with the final configuration (i.e., landing gear down and flaps 20°) set as late as possible, or in other words, at a low airspeed. The latest point of time, in order to be fully configured at the stabilisation height, is defined by the extension time needed to deploy the landing gear and flaps 20°. This extension time needs to be smaller than the flight time needed between the configuration point of the landing gear and reaching the stabilisation height (commonly 1000 ft AAL), while decelerating down to the reference speed (V_{REF}). Please note, in this example flaps 20° is defined to be selected as soon as the landing gear is extended. For this reason, the configuration points for flaps 20° and the landing gear are linked. While adjusting the configuration points for flaps 20° and the landing gear, flaps 12° is set at the highest permitted airspeed for this flap setting, called the maximum flap extended speed (V_{FE}). This allows first to adjust the flaps 20° and landing gear and extension stepwise by increasing the configuration speed until a continuous deceleration segment with flaps 12° is possible. As soon as a continuous deceleration with flaps 12° is possible, the configuration airspeeds for flaps 20° and the landing gear are fixed (—). The other continuous lines (—) in the figures show the exemplary stepwise increases of the configuration airspeed (+10 kt) starting at V_{REF} plus 10 kt. The airspeed profiles and the speed increase in the runway direction of the continuous lines may look unfamiliar. The reason for this is the declining deceleration capability at low airspeeds when using flaps 12°, which is a results of the aircraft's aerodynamics, and the use of a reverse simulation. Please keep in mind that this is an example to explain the principle of the adjustment of the configuration points. In flight operations, flaps 12° is probably not used at such low airspeeds, especially not for decelerating. Once the final landing configuration (i.e., landing gear and flaps 20°) has been adjusted and fixed, the configuration airspeed for flaps 12° is adjusted. The configuration airspeed for flaps 12° is stepwise reduced, starting at V_{FE}, and the airspeed profile changes accordingly. The dashed lines (- - -) in the figure show the stepwise decreases of the configuration airspeed (-5 kt). Once the configuration speed for flaps 12° becomes lower, the deceleration in clean configuration needs to begin earlier and the deceleration

CC BY-NC-ND 4.0

point moves accordingly in the opposite flight direction. If the configuration airspeed for flaps 12° becomes too low, the airspeed temporarily increases again while being in clean configuration. The resulting configuration airspeed for flaps 12° corresponds to the lowest airspeed possible that still allows to maintain the continuous deceleration with flaps 12° (- - -). Finally, the configuration speeds for flaps and landing gear are determined and allow a continuous deceleration with minimum engine power and being stabilised at the stabilisation height (here 1000 ft AAL).

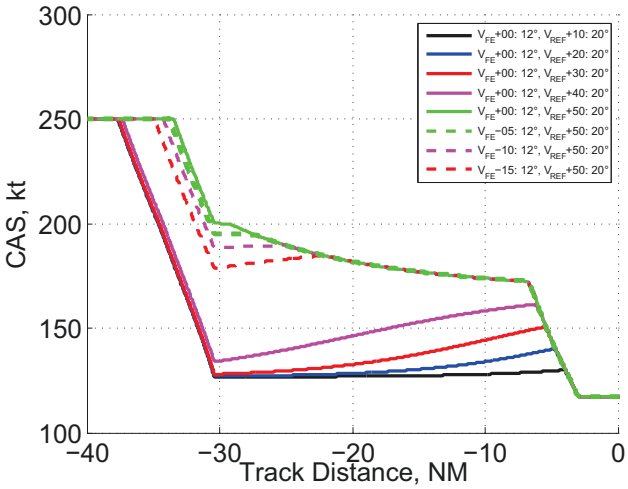


FIG 11. Optimisation algorithm principle: Calibrated airspeed profiles for various configuration speeds (i.e., flaps 12°, landing gear, and flaps 20°) for a -3° descent starting at 10,000 ft at around 30 NM, between the initial (—) and the optimised (- - -) profiles

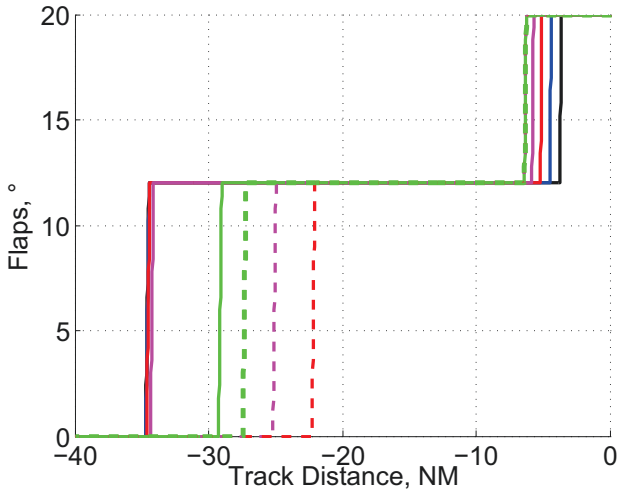


FIG 12. Optimisation algorithm principle: Flap deflection profiles for various configuration speeds (i.e., flaps 12°, landing gear, and flaps 20°) for a -3° descent starting at 10,000 ft at around 30 NM, between the initial (—) and the optimised (- - -) profiles

4.3. Requirements

The trajectory optimisation requires a flight performance model and aircraft-specific operational information, such as limitations, operational speeds, and flight procedures.

4.3.1. Flight performance model

The flight performance model used for the optimisation should be able to map the flight performance in space,

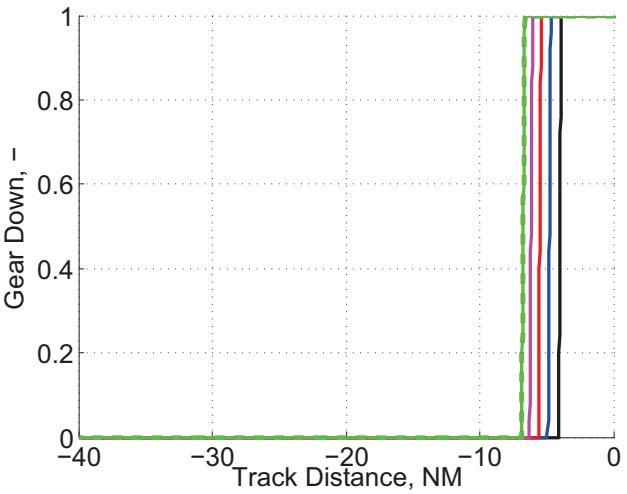


FIG 13. Optimisation algorithm principle: Landing gear profiles for various configuration speeds (i.e., flaps 12°, landing gear, and flaps 20°) for a -3° descent starting at 10,000 ft at around 30 NM, between the initial (—) and the optimised (- - -) profiles

but for a first step at least in the vertical plane. Point mass models are considered sufficient for this purpose, given by, e.g., a classical model 3 degree-of-freedom formulation containing, kinematic equations, aerodynamic coefficients, and engine thrust tables. To calculate the flight performance, the aerodynamic coefficients for each flap configuration with/without landing gear are required. These coefficients must also be available for different pressure altitudes, outside temperatures, centre of gravity positions, and for the entire speed range relevant for the approach[4]. The engine data must also be available for the relevant speeds and the different power settings so that thrust and fuel flow can be determined. In addition to the dependency on the outside temperature, the pressure altitude, and the airspeed, the bleed air extraction should also be represented. Quantitatively, no statement can be made regarding the accuracy at the present time, but a high model accuracy is preferred.

4.3.2. Operational information

For the flight phase between the top of descent and the deceleration point, the operational airspeeds of the flight manual are used for the descent. The standard configuration speeds, flight altitudes, or waypoints at which the flaps and the landing gear are configured must be available as a starting point. The flight techniques for the approach and landing of the Dornier 328-100 [19] suggest to set flaps 12° between 140 to 170 kt. The final configuration (i.e., flaps 20° or 32° and gear down) should be set shortly before glideslope intercept or at the final approach fix, depending on the type of approach (i.e., precision approach, non-precision approach). When landing with flaps 32°, flaps 20° should be set a bit earlier than the final configuration. Furthermore, the stalling speeds and the maximum flaps extended speeds must be known, to ensure that the aircraft operates within its permitted envelope.

[4] the centre of gravity and the speed range are necessary to provide information about the trimmed flight conditions

CC BY-NC-ND 4.0

5. COCKPIT DISPLAY CONCEPT

Figure 14 shows a first design of the cockpit display elements for the indication of the commands of the trajectory optimisation and to provide information to the cockpit crew. The display elements should be reduced to a minimum and integrated into the primary cockpit displays (i.e., primary flight display (PFD), multifunction display (MFD), and electronic indicating, caution, and advisory system display (EICAS)). The given information (left side in Fig. 14) includes the current target flap position (here flaps 10°), landing gear position, and the predicted speed deviation from the landing speed at the stabilisation height (here -5 kt). Colour coding indicates whether a stable or non-stable approach (green/red) is predicted at the stabilisation height.

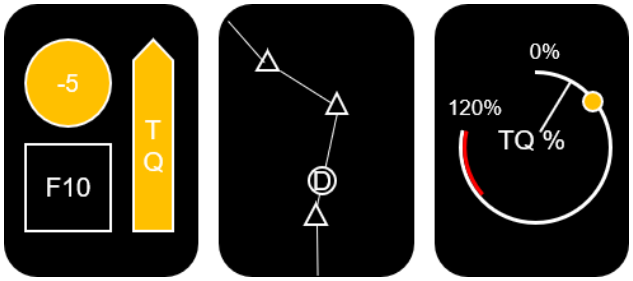


FIG 14. Cockpit display elements for the indication of system commands and information

In the event that the total energy becomes too low, so that an energy supply is required by actuating the power lever, the colour coding yellow is used and the lever actuation is additionally visualised by a yellow arrow (TQ). In addition, the required engine power in per cent is indicated by a yellow marker in the engine's torque indication (right side in Figure 14). This engine torque marker could be easily integrated directly into the existing engine torque indication in the primary engine display section of the EICAS display (right side in Fig. 14). The required level of engine power can be determined, for example, by a specific time within which a sufficient energy level shall be restored. If the total energy of the aircraft is high enough again, the indications described for this state disappear. The expected airspeed deviation at the stabilisation height should then be within an acceptable margin again and the colour coding changes back to green accordingly.

In case that the total aircraft energy is high enough or too high, the torque arrow disappears (left side in Fig. 14) and the torque marker on the primary engine display (right side in Fig. 14) stays at the minimum engine torque position to avoid further energy supply. The already existing energy excess can only become dissipated by an earlier deployment – as initially planned – of flaps and landing gear, as there are no speed brakes available and a given vertical flight trajectory needs to be flown. Therefore, the maximum energy dissipation can be reached with deploying the flaps and landing gear at their highest allowed airspeeds (i.e., V_{FE} for flaps, V_{LE}/V_{LO} for landing gear). If the aircraft can no longer get rid of the energy and a stable approach is not possible, the expected airspeed deviation at the stabilisation height (left side in Fig. 14) exceeds an acceptable margin and the colour coding changes to red. In this situation, the cockpit crew can either abort the approach, accept an airspeed overshot at the stabilisation height and thus also a non-stable approach, or adjust the vertical flight trajectory appropriately.

The points determined by the trajectory optimisation for the top of descent, deceleration point, and for the configuration of the flaps and landing gear are also shown as virtual waypoints along the existing lateral flight route on the MFD (e.g., for the deceleration point (D) in centre of Fig. 14).

Figure 15 shows an alternate display concept for manual flight without an autopilot integrated into the PFD, which differs from the concept introduced with Fig. 14. This concept for manual flight requires a pitch or attitude indicator that enables the cockpit crew to follow the desired trajectory. The function of this indicator is very similar to a usual flight director. The desired aircraft attitude (i.e., pitch and roll angle) is displayed on the artificial horizon, so that the cockpit crew can follow the trajectory by controlling the actual aircraft attitude as indicated by the fixed aircraft symbol. The desired attitude in Fig. 15 close to the fixed aircraft symbol is coloured in green. All other command cues with its target and current commands (i.e., engine torque setting, flaps, and landing gear) and additional information (i.e., airspeed deviation (here "+3" next to the attitude indicator) at the stabilisation height) are integrated into the PFD as well. The alternate display concept shows the basic design, which information are displayed and how they could be arranged, without a final colour coding or realisation of the indication elements. This is part of the current investigation. The pitch indicator and all other cues and information can be implemented the same way into the cross point flight director.

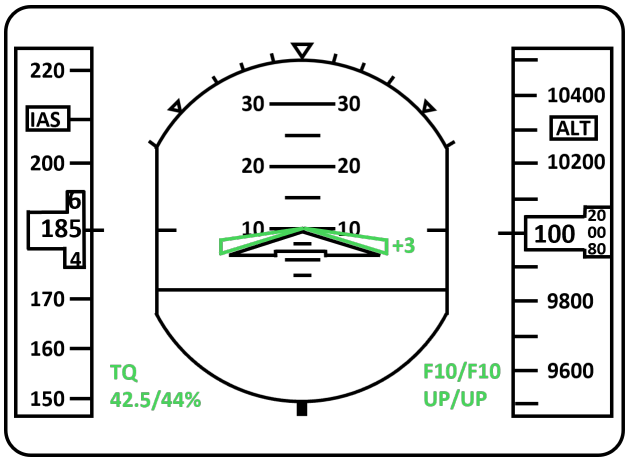


FIG 15. Cockpit system indications on the PFD for manual flight using a pitch indicator, engine torque, and aircraft configuration commands

6. DISCUSSION

The proposed trajectory optimisation methodology was developed to reduce fuel consumption and aircraft noise by providing an energy-optimised vertical flight trajectory. The energy management algorithm continuously updates the speed and configuration management to the latest aircraft states and conditions (e.g., aircraft's energy level, approach procedure, ATC instructions, changed wind conditions). The quantitative effect on fuel and noise exposure on ground is not assessed yet and has to be evaluated with fast-time simulations and (simulator) flight trials in future work. Nevertheless, the ADS-B data analysis suggests that with such a trajectory optimisation system and its recommendations for the cockpit crew, on the one hand the airspeed profiles could be smoothed and bundled or the scattering reduced, and on the other hand the energy supply from the engines could be kept to a minimum. Furthermore, the trajectory

CC BY-NC-ND 4.0

optimisation and the displayed recommendations for actions should make it easier to avoid individual approaches with too much or too low energy. The effects mentioned may result in a reduction in fuel consumption and noise exposure on ground. A prerequisite is that the cockpit crews can follow the trajectory with sufficient accuracy. The fuel and noise reductions are to be expected on average, even though individual pilots may well be able to fly with comparable or even less fuel or noise.
The proposed optimisation methodology for the turboprop aircraft used (Dornier 328-100) is based on a predefined fix sequence of aircraft configurations (i.e., flaps and landing gear). However, the aircraft type and predefined procedural steps are generally adjustable. The trajectory optimisation system function is limited to the predefined procedural steps and it is not intended to be used, for example, for abnormal or emergency procedures. Furthermore, the trajectory optimisation methodology is currently limited to RNP approaches, as the energy management algorithm requires a flight path angle along the entire lateral flight path. This is due to the lack of detailed information on the exact aircraft-side implementation of the autopilot's vertical flight modes. As soon as this information is available in the future and can also be modelled by the trajectory optimisation system, the concept could also be adapted to other procedures. Even if only the flight trajectory in the vertical plane is optimised, the trajectory considered is still not limited to a straight approach, but can also take into account a curved flight path by considering the track distance to threshold and the effect of a roll angle.
The high-quality data recommended for the flight performance model are often only available from the aircraft manufacturer, even if the optimisation algorithm can calculate any results with less precise data that at least provide the required parameters.
New visual cues to display the trajectory optimisation results and its recommendations for actions, as described in Chapter 5, should be integrated into the primary cockpit displays (i.e., PFD, MFD) to achieve maximum benefit with minimal modifications on the flight deck, compared to implementing cues into an additional external display device. For a mostly manually controlled aircraft, an extension of flight director functions (if available) might be the most reasonable approach. In this case, all cues are provided within the primary field of view and placed direct to the most important flight instrument information to control the aircraft (i.e., attitude indicators, airspeed, altitude, vertical speed, and heading). Nevertheless, the choice of display indications are subject to the flight deck design and human performance considerations.

7. SUMMARY AND OUTLOOK

This paper describes a trajectory optimisation methodology for turboprop aircraft with the basic algorithms and exemplary cockpit display concepts. The aim of the trajectory optimisation is to support the cockpit crew during descent and approach to fly with minimum engine power and to ensure a stable approach. Appropriate display elements are intended to indicate the optimised times for initiating descent, the start of the deceleration, and the configuration of the flaps and landing gear.
ADS-B data were tracked and analysed to discuss potential for fuel and noise reduction, as a quantitative assessment was not yet possible. Thanks to the expected optimised speed and aircraft configuration management of the proposed trajectory optimisation, a reduction in fuel consumption is expected on average during flight operations. Furthermore, a reduction in particularly loud/extreme noise events on individual approaches is probable. As a side effect, a quieter approach and a reduction in cabin noise is also conceivable, as a continuous energy reduction with minimum engine power should be achieved. This should avoid or significantly reduce the need for (frequent) re-adjustment by the cockpit crew via the engine power lever. The function can help to continuously monitor the aircraft's current total energy state and to increase the pilots' situational awareness with regard to energy management. This could also reduce the workload in a labour-intensive flight phase and reduce the number of non-stable approaches. This could be particularly helpful at new aerodromes or for particularly challenging approaches, such as steeper approach angles.
The development of the trajectory optimisation algorithm for the methodology presented has not yet been completed and testing is still pending. As soon the trajectory optimisation function is developed and implemented, the quantitative effects on fuel consumption and noise levels on ground will be determined by comparing approaches with and without the trajectory optimisation. The pilot campaign in the simulator planned in near future and the subsequent noise calculations will provide information on this. Furthermore, the subjective effectiveness with regard to energy management and the supporting display elements during the approach will be evaluated by (test) pilots. Their preferences with regard to aspects such as usability and effectiveness of the display concept will be evaluated by questionnaires. The feedback and knowledge gained from the simulator campaign might be highly valuable for the further development of trajectory optimisation for turboprop aircraft in order to adapt the system function as best as possible to the flight operational requirements, the needs of the pilots, and in terms of practicability. It is also conceivable that the tests will reveal new potentials that were not previously visible and/or could not be realised without flight operations data and without relevant experience with turboprop aircraft.
The discussion of the ADS-B data analysis suggests that the implementation of an auto-throttle system could provide further potential to improve airspeed stability, increase energy efficiency, and to reduce engine noise.
In 2026, a flight test campaign is planned to measure noise levels of DLR's UpLift Dornier 328-100 research turboprop aircraft (D-CUPL) and to develop a precise turboprop aircraft noise model. This noise model will allow to precisely calculate and assess the effect of trajectory optimisation on noise exposure on ground.

Contact address:

joscha.kurz@dlr.de

Funding Information

The work is part of the project *Clean Aviation via Intelligent Avionics* (LuFo-Förderkennzeichen 20X2202B), which is supported by the Federal Ministry for Economic Affairs and Energy on the basis of a decision by the German Bundestag.

CC BY-NC-ND 4.0

References

[1] European Environment Agency and European Union Aviation Safety Agency. European Aviation Environmental Report 2025, 2025. DOI: 10.2822/1537033, https://www.easa.europa.eu/sites/default/files/eaer-downloads/EASA_EAER_2025_Book_v5.pdf.

[2] European Environment Agency and European Union Aviation Safety Agency. European Aviation Environmental Report 2022, 2022. DOI: 10.2822/04357, https://data.europa.eu/doi/10.2822/04357.

[3] European Environment Agency and European Union Aviation Safety Agency. European Aviation Environmental Report 2019, 2019. DOI: 10.2822/309946, https://data.europa.eu/doi/10.2822/309946.

[4] World Health Organization. *Environmental Noise Guidelines for the European Region*. World Health Organization, Regional Office for Europe, Copenhagen, Denmark, 2018. ISBN: 978 92 890 5356 3.

[5] European Commission. *Flightpath 2050: Europe's vision for aviation; maintaining global leadership and serving society's needs; report of the High-Level Group on Aviation Research*. Policy / European Commission. Publ. Off. of the Europ. Union, Luxembourg, 2011. ISBN: 978-92-79-19724-6.

[6] International Civil Aviation Organization. Guidance on the Balanced Approach to Aircraft Noise Management, 2008. https://www.bazl.admin.ch/dam/bazl/de/dokumente/Fachleute/Flugplaetze/ICAO/icao_doc_9829_guidanceonthebalancedapproachtoaircraftnoisemanage.pdf.download.pdf/icao_doc_9829_guidanceonthebalancedapproachtoaircraftnoisemanage.pdf.

[7] Marco Scholz and Fethi Abdelmoula. Active Noise Abatement Using the Newly Developed Pilot Assistance System LNAS. In *INTER-NOISE 2017*, Hong Kong, China, August 2017.

[8] Tobias Bauer, Fethi Abdelmoula, Johan Boyer, Martin Gerber, Jonas Meister, and Jean Marc Wunderli. Improved Configuration Management for Greener Approaches – Evaluation of a Novel Pilot Support Concept. In *33rd Congress of the International Council of the Aeronautical Sciences, ICAS 2022*, November 2022.

[9] C. G. Kühne, M. Scholz, F. Abdelmoula. LNAS – A Pilot Assistance System for Energy-Optimal Approaches Using Existing Aircraft-Infrastructure. In *AEGATS 2018*, Toulouse, France, 2018.

[10] Fethi Abdelmoula and Marco Scholz. LNAS - A Pilot Assistance System for Low-Noise Approaches With Minimal Fuel Consumption. In *31st Congress of the International Council of the Aeronautical Sciences*, Belo Horizonte, Brasil, 2018.

[11] David Jäger, Christoph Zellmann, Jean Marc Wunderli, Marco Scholz, Fethi Abdelmoula, and Martin Gerber. Validation of an airline pilot assistant system for low-noise approach procedures. *Transportation Research Part D: Transport and Environment*, 99:103020, 2021. ISSN: 1361-9209. DOI: https://doi.org/10.1016/j.trd.2021.103020.

[12] Martin Gerber, York Schreiber, Fethi Abdelmoula, Christoph G. Kühne, D. Jäger, and J. M. Wunderli. Energy-optimized approaches: a challenge from the perspectives of pilots and air traffic controllers. *CEAS Aeronautical Journal*, 13(4):1055–1066, Sept. 2022. ISSN: 1869-5590. DOI: 10.1007/s13272-022-00607-0.

[13] Martin Gerber, Marie Goetz, Falk Sachs, Peter Pauly, and Fethi Abdelmoula. Improving Aircraft Energy and Flightpath Management: Demonstration of Optimized Continuous Descent Approaches with A320neo in regular Operation Along A Closed-Path PBN-To-ILS Transition using a Pilot Assistance System at Zurich Airport. In *Deutscher Luft- und Raumfahrtkongress*, Hamburg, Oktober 2024.

[14] Falk Sachs, Fethi Abdelmoula, Marie Goetz, and Joscha Kurz. Trials for quiet and efficient flights in advanced continuous descent approach using the low-noise augmentation system LNAS. *CEAS Aeronautical Journal*, Mar. 2025. ISSN: 1869-5590. DOI: 10.1007/s13272-025-00825-2.

[15] Willy J.G. Bräunling. *Flugzeugtriebwerke: Grundlagen, Aero-Thermodynamik, ideale und reale Kreisprozesse, Thermische Turbomaschinen, Komponenten, Emissionen und Systeme*. Springer Berlin Heidelberg, 2015. ISBN: 9783642345395. DOI: 10.1007/978-3-642-34539-5.

[16] Deutsche Aircraft GmbH. Airplane Operating Manual (Volume 2) - Dornier 328-100, 2023.

[17] H. Hersbach, B. Bell, P. Berrisford, G. Biavati, A. Horányi, J. Muñoz Sabater, J. Nicolas, C. Peubey, R. Radu, I. Rozum, D. Schepers, A. Simmons, C. Soci, D. Dee, and J-N. Thépaut. ERA5 hourly data on pressure levels from 1940 to present, 2023. DOI: 10.24381/CDS.BD0915C6.

[18] 328 Support Services GmbH. Airplane Flight Manual - Dornier 328-100, 2021.

[19] Deutsche Aircraft GmbH. Airplane Operating Manual (Volume 1) - Dornier 328-100, 2023.

[20] Deutsche Aircraft GmbH. Quick Reference Handbook - Dornier 328-100, 2022.

[21] Rudolf Brockhaus, Wolfgang Alles, and Robert Luckner. *Flugregelung*. Springer-Verlag Berlin Heidelberg, Berlin, Heidelberg, 3th edition, 2011. ISBN: 978-3-642-01442-0.

CC BY-NC-ND 4.0